



香港城市大學
City University of Hong Kong

專業 創新 胸懷全球
Professional · Creative
For The World

CityU Scholars

Photofunctional cyclometallated iridium(III) polypyridine methylsulfone complexes as sulfhydryl-specific reagents for bioconjugation, bioimaging and photocytotoxic applications

Huang, Lili; Leung, Peter Kam-Keung; Lee, Lawrence Cho-Cheung; Xu, Guang-Xi; Lam, Yun-Wah; Lo, Kenneth Kam-Wing

Published in:
Chemical Communications

Published: 18/09/2022

Document Version:
Post-print, also known as Accepted Author Manuscript, Peer-reviewed or Author Final version

Publication record in CityU Scholars:
[Go to record](#)

Published version (DOI):
[10.1039/d2cc02405e](https://doi.org/10.1039/d2cc02405e)

Publication details:
Huang, L., Leung, P. K-K., Lee, L. C-C., Xu, G-X., Lam, Y-W., & Lo, K. K-W. (2022). Photofunctional cyclometallated iridium(III) polypyridine methylsulfone complexes as sulfhydryl-specific reagents for bioconjugation, bioimaging and photocytotoxic applications. *Chemical Communications*, 58(73), Article 10162. Advance online publication. <https://doi.org/10.1039/d2cc02405e>

Citing this paper

Please note that where the full-text provided on CityU Scholars is the Post-print version (also known as Accepted Author Manuscript, Peer-reviewed or Author Final version), it may differ from the Final Published version. When citing, ensure that you check and use the publisher's definitive version for pagination and other details.

General rights

Copyright for the publications made accessible via the CityU Scholars portal is retained by the author(s) and/or other copyright owners and it is a condition of accessing these publications that users recognise and abide by the legal requirements associated with these rights. Users may not further distribute the material or use it for any profit-making activity or commercial gain.

Publisher permission

Permission for previously published items are in accordance with publisher's copyright policies sourced from the SHERPA RoMEO database. Links to full text versions (either Published or Post-print) are only available if corresponding publishers allow open access.

Take down policy

Contact lbscholars@cityu.edu.hk if you believe that this document breaches copyright and provide us with details. We will remove access to the work immediately and investigate your claim.

This journal is © The Royal Society of Chemistry 2022.

This is the accepted version of a paper published in *Chemical Communications*. This paper has been peer-reviewed but does not include the final publisher proof-corrections or journal pagination.

Huang, L., Leung, P. K-K., Lee, L. C-C., Xu, G-X., Lam, Y-W., & Lo, K. K-W. (2022). Photofunctional cyclometallated iridium(III) polypyridine methylsulfone complexes as sulfhydryl-specific reagents for bioconjugation, bioimaging and photocytotoxic applications. *Chemical Communications*, 58(73), [10162].

<https://doi.org/10.1039/d2cc02405e>.

COMMUNICATION

Photofunctional cyclometallated iridium(III) polypyridine methylsulfone complexes as sulfhydryl-specific reagents for bioconjugation, bioimaging and photocytotoxic applications†

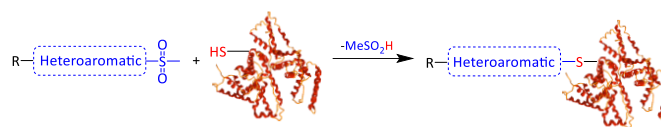
Received 00th January 20xx,
Accepted 00th January 20xx

DOI: 10.1039/x0xx00000x

Lili Huang,^a Peter Kam-Keung Leung,^{ab} Lawrence Cho-Cheung Lee,^{ac} Guang-Xi Xu,^a Yun-Wah Lam^{*a} and Kenneth Kam-Wing Lo^{*ab}

We report herein near-infrared (NIR)-emitting cyclometallated iridium(III) complexes bearing a heteroaromatic methylsulfone moiety as sulfhydryl-specific reagents; one of the complexes was conjugated to cysteine and cysteine-containing peptides and proteins for bioimaging and photocytotoxic applications.

Bioconjugation offers valuable opportunities to label specific biomolecules, such as peptides and proteins, with functional groups for bioimaging and therapeutic applications.¹ Among different amino acids, cysteine is a highly favourable handle for selective conjugation due to its relatively low natural abundance (< 2%) and the highly nucleophilic sulfhydryl side-chain.² Recently, heteroaromatic methylsulfones have emerged as a new class of electrophiles for selective sulfhydryl modification via nucleophilic aromatic substitution, forming a heteroaryl–thiol linkage in proteins (Scheme 1).³ These methylsulfone-containing reagents display high reactivity and selectivity toward sulfhydryl over other reactive functionalities such as amines, sulfenic acids and S-nitrosothiols under mild conditions, compared to widely used thiol-modifying reagents such as maleimide and haloacetamide.⁴ The reactivity of heteroaromatic methylsulfones toward sulfhydryl can be further enhanced through the introduction of electron-withdrawing groups such as carboxylic acid and nitro moieties.³ Additionally, the heteroaryl–thiol linkage formed exhibits much higher stability than the thioether linkage in maleimide–thiol conjugates in the presence of acids, bases or external thiols.⁵ Thus, methylsulfone-containing reagents have received considerable attention as labels for peptides and proteins,⁵ for the preparation of antibody–drug conjugates,⁶ and for the detection and imaging of thiol species in live cells.⁷



Scheme 1 Labeling of cysteine residues of proteins by heteroaromatic methylsulfones.

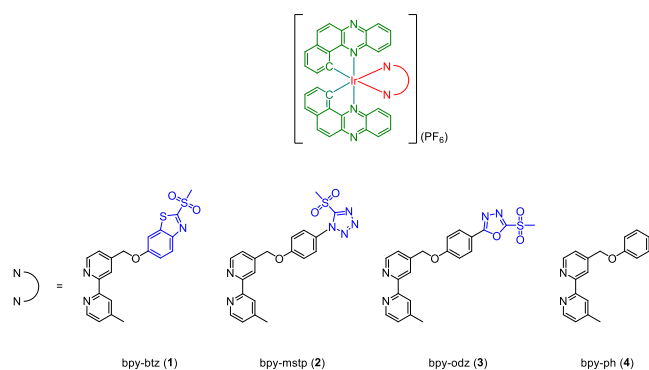
In the past decade, there has been emerging interest in the development of transition metal–peptide conjugates for bioimaging, biosensing and therapeutic applications.⁸ Luminescent transition metal complexes such as cyclometallated iridium(III) complexes typically possess many advantages such as their tuneable emission energies, long emission lifetimes, high photostability and high singlet oxygen (¹O₂)-photosensitisation capability.⁹ These complexes have been conjugated to peptides such as cell-penetrating,¹⁰ organelle-targeting¹¹ and receptor-targeting peptides¹² to modulate their cellular uptake and intracellular localisation properties. Metal–peptide conjugates are commonly prepared from the coupling of a metal complex to a resin-bound, protected peptide, followed by peptide cleavage and deprotection to achieve site-selective functionalisation.¹³ Also, selective post-modification of an unprotected peptide with a metal complex under mild and biocompatible conditions is highly attractive.¹⁴ With our continued effort in the design of sulfhydryl-specific reagents,^{14d, e, 15} we report herein the design and synthesis of three near-infrared (NIR)-emitting cyclometallated iridium(III) polypyridine complexes modified with a heteroaromatic methylsulfone moiety [Ir(bpz)₂(N[^]N)](PF₆) (Hbpz = benzo[*a*]phenazine; N[^]N = bpy-btz (**1**), bpy-mstp (**2**) and bpy-odz (**3**)) (Scheme 2) for the chemoselective modification of cysteine. The methylsulfone-free analogue [Ir(bpz)₂(bpy-ph)](PF₆) (**4**) was also prepared for comparison (Scheme 2). The development of NIR-emissive probes is highly important for biomedical imaging as luminescent probes with absorption and emission in the visible region ($\lambda < 650$ nm) are usually limited by short tissue penetration and interference by the strong autofluorescence background. Thus, the ligand Hbpz with a high degree of π -conjugation was selected as a cyclometalating ligand with the purpose of tuning the emission of the complexes to the NIR region. The synthetic procedures and characterisation data are included in the ESI.[†]

^a Department of Chemistry, City University of Hong Kong, Tat Chee Avenue, Hong Kong, P. R. China.

^b State Key Laboratory of Terahertz and Millimetre Waves, City University of Hong Kong, Tat Chee Avenue, Kowloon, Hong Kong, P. R. China.

^c Laboratory for Synthetic Chemistry and Chemical Biology Limited, Units 1503 – 1511, 15/F, Building 17W, Hong Kong Science Park, New Territories, Hong Kong, P. R. China.

† Electronic Supplementary Information (ESI) available. See DOI: 10.1039/x0xx00000x



Scheme 2 Structures of complexes 1 – 4.

All the complexes displayed intense spin-allowed singlet intraligand (¹IL) ($\pi \rightarrow \pi^*$) (N^{^N} and bpz) absorption at *ca.* 275 – 410 nm and weaker spin-allowed metal-to-ligand charge-transfer (¹MLCT) ($d\pi(\text{Ir}) \rightarrow \pi^*(\text{N}^{\wedge}\text{N}$ and bpz)) absorption features at *ca.* 411 – 630 nm (Table S1 and Fig. S1). The weaker absorption tailing beyond *ca.* 631 nm is assigned to spin-forbidden ³MLCT ($d\pi(\text{Ir}) \rightarrow \pi^*(\text{N}^{\wedge}\text{N}$ and bpz)) transitions. Upon photoexcitation, all the complexes exhibited intense and long-lived deep-red emission (Table 1 and Fig. S2). The long emission lifetimes and insensitivity of emission properties to solvent polarity indicate that the emission originates from a predominant ³IL ($\pi \rightarrow \pi^*$) (bpz) state. This is supported by the vibrationally structured emission bands and long emission lifetimes (8.30 – 9.91 μs) in 77-K glass. Additionally, the ¹O₂ generation quantum yields (Φ_{Δ}) of the complexes were determined in aerated MeOH using 1,3-diphenylisobenzofuran (DPBF) as a ¹O₂ scavenger (Table 1). The Φ_{Δ} values of complexes 1 – 3 (0.77 – 0.89) were comparable to that of complex 4 (0.82), indicating that the methylsulfone moiety did not influence the photophysical and photochemical properties of the iridium(III) polypyridine unit.

Table 1 Photophysical data and ¹O₂ generation quantum yields (Φ_{Δ}) of complexes 1 – 4.

Complex	Medium (T/K)	λ_{em}/nm^a	$\tau_0/\mu\text{s}^b$	Φ_{em}^c	Φ_{Δ}^d
1	CH ₂ Cl ₂ (298)	664	5.63	0.085	0.79
	CH ₃ CN (298)	668	3.26	0.044	
	Glass ^e (77)	663, 726 sh	8.30		
2	CH ₂ Cl ₂ (298)	664	5.34	0.085	0.89
	CH ₃ CN (298)	668	3.46	0.048	
	Glass ^e (77)	663, 726 sh	9.91		
3	CH ₂ Cl ₂ (298)	664	5.08	0.072	0.77
	CH ₃ CN (298)	668	3.23	0.044	
	Glass ^e (77)	663, 726 sh	9.40		
4	CH ₂ Cl ₂ (298)	664	5.12	0.068	0.82
	CH ₃ CN (298)	668	3.44	0.052	
	Glass ^e (77)	663, 726 sh	9.22		

^a λ_{ex} = 350 nm. ^b The lifetimes were measured at the emission maxima (λ_{ex} = 355 nm). ^c [Ru(bpy)₃]Cl₂ was used as a reference (Φ_{em} = 0.04 in aerated H₂O).¹⁶ ^d [Ru(bpy)₃]Cl₂ in aerated MeOH was used as a reference (Φ_{Δ} = 0.73).¹⁷ ^e EtOH/MeOH (4:1, v/v).

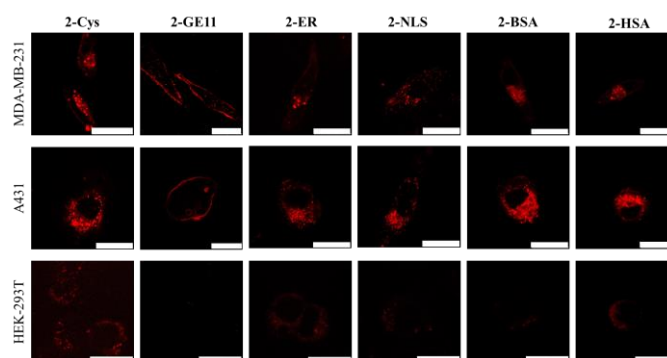


Fig. 1 LSCM images of MDA-MB-231, A431 and HEK-293T cells incubated with **2-Cys**, **2-GE11**, **2-ER**, **2-NLS**, **2-BSA** and **2-HSA** (10 μM , 4 h, λ_{ex} = 488 nm, λ_{em} = 650 – 750 nm). Scale bar = 25 μm for MDA-MB-231 and A431, and 10 μm for HEK-293T.

The reactivity of the methylsulfone complexes 1 – 3 toward L-cysteine in aqueous solutions was analysed by reversed-phase high-performance liquid chromatography (RP-HPLC). The complexes (25 μM) were incubated with cysteine (250 μM) in potassium phosphate buffer (100 mM, pH 8.0)/DMF (4:1, v/v, 500 μL) containing tris(2-carboxyethyl)phosphine (TCEP) (750 μM) at 37°C. Complexes 2 and 3 reacted rapidly with cysteine (< 5 min) to afford the iridium(III)–cysteine conjugates **2-Cys** and **3-Cys**, respectively, with reaction yields > 98%. However, it took much longer for complex 1 to complete the same reaction (2 h, Fig. S3). The formation of products was confirmed by ESI-MS (Fig. S4). The second-order rate constants (k_2) of the reaction of complexes 1, 2 and 3 with cysteine were determined to be *ca.* 1.4, 83.6 and 1228.4 $\text{M}^{-1} \text{s}^{-1}$, respectively (Fig. S5), which are similar to those of the corresponding free ligands (k_2 = 1.6, 79.5 and 1033.2 $\text{M}^{-1} \text{s}^{-1}$, respectively) (Fig. S6). Thus, the metal complex cores did not substantially affect the reactivity of the heteroaromatic methylsulfone group, which is in line with the fact that there is a lack of π -conjugated linker between the two units. Although complex 3 displayed the highest reactivity toward cysteine, it was also more susceptible to hydrolysis (Fig. S7). Thus, complex 2, which exhibited a delicate balance of high reactivity and stability, was selected as a model complex for further studies.

Complex 2 was incubated with amino acids bearing reactive side-chains such as L-lysine, L-histidine and L-serine for 12 h under the same conditions mentioned above. No reactions were observed, illustrating the high chemoselectivity of the complex toward cysteine (Fig. S8). Next, an epidermal growth factor receptor (EGFR)-targeting peptide modified with a cysteine residue at the N-terminus CYHWYGYTPQNV (GE11)¹⁸ was employed as a model for conjugation studies. Upon the incubation of GE11 (250 μM) and complex 2 (25 μM) in potassium phosphate buffer (100 mM, pH 8.0)/DMF (4:1, v/v, 500 μL) containing TCEP (750 μM) at 37°C for 30 min, the production of the peptide conjugate **2-GE11** was confirmed by RP-HPLC and ESI-MS (Fig. S9 and S13). Given the high reactivity, selectivity and stability of complex 2, it was also conjugated to cysteine-modified endoplasmic reticulum-targeting peptide CKDEL (ER) and nuclear localisation sequence CPKKRKV (NLS), and the proteins bovine serum albumin (BSA) and human serum albumin (HSA) to afford conjugates **2-ER**, **2-NLS**, **2-BSA** and **2-HSA**, respectively. All the conjugates were purified by RP- or size-exclusion HPLC, and their photophysical and photochemical properties were studied. Upon irradiation, the peptide conjugates displayed moderately intense and

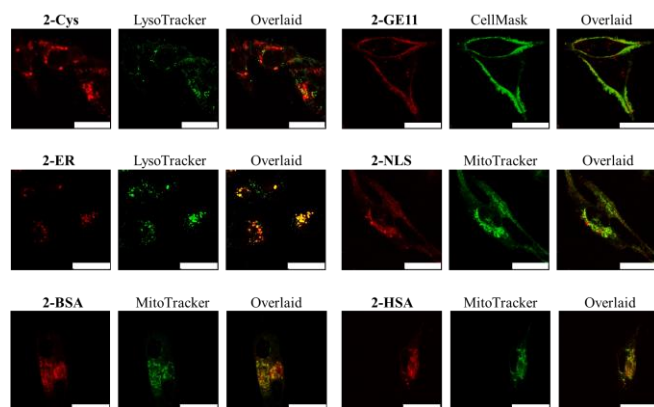


Fig. 2 LSCM images of MDA-MB-231 cells incubated with **2-Cys**, **2-GE11**, **2-ER**, **2-NLS**, **2-BSA** and **2-HSA** (10 μ M, 4 h, λ_{ex} = 488 nm, λ_{em} = 650 – 750 nm) at 37°C and then with an organelle stain (LysoTracker Green, 100 nM, 20 min, λ_{ex} = 488 nm, λ_{em} = 506 – 526 nm; MitoTracker Green, 100 nM, 20 min, λ_{ex} = 488 nm, λ_{em} = 506 – 526 nm; CellMask Deep Red, 5 μ g/mL, 10 min, λ_{ex} = 635 nm, λ_{em} = 650 – 700 nm) at 37°C. Scale bar = 25 μ m.

long-lived emission and high Φ_{Δ} (0.61 – 0.86) (Table S2), showing that the conjugation did not significantly perturb the photophysical and photochemical behaviour of the complexes. The emission maxima of **2-BSA** and **2-HSA** were blue-shifted, and their emission lifetimes were longer and quantum yields were higher than those of the peptide conjugates, which are ascribed to the hydrophobic local environments of the complexes after conjugation to the protein molecules.^{15d} The Φ_{Δ} values of the two protein conjugates (0.17 and 0.11) were smaller than those of the peptide conjugates (0.61 – 0.86), which may be due to the entrapment of 1O_2 in the protein matrix, rendering it more difficult to diffuse out and react with DPBF.

The intracellular localisation properties of the peptide and protein conjugates of complex **2** and the methylsulfone-free complex **4** were investigated by laser-scanning confocal microscopy (LSCM) using MDA-MB-231 (breast carcinoma), A431 (epidermoid carcinoma) and HEK-293T (normal human embryonic kidney) cells as models (Fig. 1 and S19). In general, all six conjugates showed stronger luminescence signals in MDA-MB-231 and A431 cells than in HEK-293T cells (Fig. 1), but there was no noticeable difference for complex **4** (Fig. S19). Incubation of MDA-MB-231 cells with **2-Cys** resulted in punctate cytoplasmic staining (Fig. 1). Very weak co-localisation with LysoTracker Green (Pearson's correlation coefficient (PCC) = 0.37) (Fig. 2) suggested that the conjugate was entrapped in the endosomes after uptake.¹⁹ Notably, treatment of MDA-MB-231 cells with **2-GE11** gave rise to intense emission in the

plasma membrane (Fig. 1) with strong co-localisation with CellMask Deep Red (PCC = 0.88) (Fig. 2). This is most likely resulted from the affinity of the GE11 peptide with EGFRs on the cell surface.²⁰ Cells incubated with **2-ER** and **2-NLS** showed intense emission in the lysosomal (PCC = 0.73) and mitochondrial (PCC = 0.82) regions, respectively, instead of the expected endoplasmic reticulum and nucleus. The localisation of **2-ER** in the lysosomes can be ascribed to the entrapment of the conjugate in these organelles, while the mitochondrial enrichment of **2-NLS** may be due to the cationic and lipophilic character of the conjugate.^{14e} The perinuclear staining by the protein conjugates **2-BSA** and **2-HSA** in the cell lines suggests their localisation in the mitochondrial region, which was confirmed by co-staining experiments (Fig. 2). Complex **4** was also localised in the mitochondria of MDA-MB-231 cells (Fig. S19 and S20).

The cytotoxicity of the six conjugates and complex **4** was studied by the 3-(4,5-dimethylthiazol-2-yl)-2,5-diphenyltetrazolium bromide (MTT) assay. All six conjugates showed relatively low cytotoxic activity toward the three cell lines in the dark ($IC_{50,dark} > 20 \mu$ M) after an incubation period of 4 h (Table 2).²¹ However, upon irradiation (450 nm, 10 mW cm^{-2}) for 20 min, their cytotoxicity was substantially enhanced ($IC_{50,light} = 0.07 - 10.09 \mu$ M). Notably, the four peptide conjugates **2-Cys**, **2-GE11**, **2-ER** and **2-NLS** displayed potent photocytotoxic activity toward cancerous MDA-MB-231 and A431 cells ($IC_{50,light} = 0.07 - 1.01 \mu$ M) with a photocytotoxicity index (PI, $IC_{50,dark}/IC_{50,light} > 20$); the activity was much higher than those toward HEK-293T cells ($IC_{50,light} = 0.44 - 10.09 \mu$ M; PI > 2). These findings are attributable to the more efficient uptake of the peptide conjugates by the cancer cells than the normal HEK-293T cells. This was supported by the ICP-MS data, which showed that the iridium content in cancer cells (1.17 – 2.62 fmol/cell) was higher than in normal cells (0.13 – 0.32 fmol/cell) (Table S4). In agreement with these results, the intracellular emission intensity of HEK-293T cells was much weaker than those of the two cancer cell lines (Fig. 1). Notably, **2-GE11** exhibited higher cancer-selective photocytotoxicity than the other conjugates, as the $IC_{50,light}$ values of this conjugate toward MDA-MB-231 (1.01 μ M) and A431 cells (0.49 μ M) was one and two orders of magnitude smaller than that toward HEK-293T cells (10.09 μ M) (Table 2), which is also in agreement with uptake data (Table S4). The protein conjugates **2-BSA** and **2-HSA** showed higher dark cytotoxicity toward the two cancer cells than the normal cells. However, a similar trend was not observed in the photocytotoxicity, which is most likely due to a combined effect of the 1O_2 quantum yields, uptake efficiency and localisation. In comparison, the methylsulfone-free complex **4** exhibited very high

Table 2 (Photo)cytotoxicity (IC_{50}) of the conjugates of complex **2** and the methylsulfone-free complex **4** toward MDA-MB-231, A431 and HEK-293T cells. The cells were first incubated with the complexes in the dark for 4 h, then washed thoroughly with PBS, incubated in the dark or irradiated at 450 nm (10 mW cm^{-2}) for 20 min, and subsequently incubated in the dark for 24 h. Photocytotoxicity index (PI) = $IC_{50,dark}/IC_{50,light}$.

Compound	MDA-MB-231			A431			HEK-293T		
	$IC_{50,dark}/\mu$ M	$IC_{50,light}/\mu$ M	PI	$IC_{50,dark}/\mu$ M	$IC_{50,light}/\mu$ M	PI	$IC_{50,dark}/\mu$ M	$IC_{50,light}/\mu$ M	PI
2-Cys	> 20	0.07 \pm 0.01	> 270	> 20	0.12 \pm 0.01	> 166	> 20	0.44 \pm 0.10	> 46
2-GE11	> 20	1.01 \pm 0.08	> 20	> 20	0.49 \pm 0.01	> 40	> 20	10.09 \pm 1.85	> 2
2-ER	> 20	0.52 \pm 0.07	> 39	> 20	0.25 \pm 0.01	> 82	> 20	3.08 \pm 0.10	> 6
2-NLS	> 20	0.11 \pm 0.01	> 187	> 20	0.13 \pm 0.01	> 156	> 20	1.27 \pm 0.12	> 16
2-BSA	46.21 \pm 3.74	0.28 \pm 0.06	168	28.36 \pm 3.40	0.17 \pm 0.01	169	49.65 \pm 6.04	0.24 \pm 0.06	204
2-HSA	53.05 \pm 2.99	0.44 \pm 0.09	120	24.91 \pm 0.20	0.13 \pm 0.01	186	74.90 \pm 3.29	0.43 \pm 0.07	174
4	0.69 \pm 0.05	0.02 \pm 0.005	41	0.49 \pm 0.04	0.005 \pm 0.001	98	0.94 \pm 0.12	0.02 \pm 0.008	47

dark and light cytotoxic activity toward the three cell lines ($IC_{50, \text{dark}} = 0.49 - 0.94 \mu\text{M}$, $IC_{50, \text{light}} = 0.005 - 0.02 \mu\text{M}$) (Table 2), which should be associated with its high uptake (Table S4) and large Φ_{Δ} (Table 1). These results indicate that bioconjugation readily modulates the cellular uptake and the (photo)cytotoxic activity of the complexes.

In conclusion, we have developed cyclometallated iridium(III) polypyridine methylsulfone complexes featuring NIR emission, high reactivity and selectivity to cysteine-bearing peptides and proteins. Bioconjugates modified with these complexes displayed different intracellular localisation properties. We believe that related transition metal methylsulfone complexes with both absorption and emission in the NIR region (e.g., by using extensively π -conjugated ligands and two-photon absorption) can be designed as attractive sulfhydryl-specific reagents for bioconjugation.

We thank the Hong Kong Research Grants Council (Project No. CityU 11300019, CityU 11302820, CityU 11301121, T42-103/16-N, C7075-21GF and N_CityU104/21) for financial support. We also thank the funding support from "Laboratory for Synthetic Chemistry and Chemical Biology" under the Health@InnoHK Program launched by Innovation and Technology Commission, The Government of Hong Kong SAR, P. R. China. Lili Huang acknowledges the receipt of a Postgraduate Studentship administered by City University of Hong Kong.

Conflicts of interest

There are no conflicts to declare.

References

- (a) N. Stephanopoulos and M. B. Francis, *Nat. Chem. Biol.*, 2011, **7**, 876 – 884; (b) N. Krall, F. P. da Cruz, O. Boutureira and G. J. L. Bernardes, *Nat. Chem.*, 2016, **8**, 103 – 113.
- (a) J. M. Chalker, G. J. L. Bernardes, Y. A. Lin and B. G. Davis, *Chem. Asian J.*, 2009, **4**, 630 – 640; (b) S. B. Gunnoo and A. Madder, *ChemBioChem*, 2016, **17**, 529 – 553; (c) F. Brotzel and H. Mayr, *Org. Biomol. Chem.*, 2007, **5**, 3814 – 3820.
- H. F. Motiwala, Y.-H. Kuo, B. L. Stinger, B. A. Palfey and B. R. Martin, *J. Am. Chem. Soc.*, 2020, **142**, 1801 – 1810.
- (a) X. Chen, H. Wu, C.-M. Park, T. H. Poole, G. Keceli, N. O. Devarie-Baez, A. W. Tsang, W. T. Lowther, L. B. Poole, S. B. King, M. Xian and C. M. Furdui, *ACS Chem. Biol.*, 2017, **12**, 2201 – 2208; (b) D. Zhang, N. O. Devarie-Baez, Q. Li, J. R. Lancaster and M. Xian, *Org. Lett.*, 2012, **14**, 3396 – 3399.
- N. Toda, S. Asano and C. F. Barbas III, *Angew. Chem. Int. Ed.*, 2013, **52**, 12592 – 12596.
- J. T. Patterson, S. Asano, X. Li, C. Rader and C. F. Barbas III, *Bioconjugate Chem.*, 2014, **25**, 1402 – 1407.
- P. Zhou, J. Yao, G. Hu and J. Fang, *ACS Chem. Biol.*, 2016, **11**, 1098 – 1105.
- (a) B. Albada and N. Metzler-Nolte, *Chem. Rev.*, 2016, **116**, 11797 – 11839; (b) S. M. Meier-Menches and A. Casini, *Bioconjugate Chem.*, 2020, **31**, 1279 – 1288; (c) L. Holden, C. S. Burke, D. Cullinane and T. E. Keyes, *RSC Chem. Biol.*, 2021, **2**, 1021 – 1049.
- (a) K. K.-W. Lo, *Acc. Chem. Res.*, 2015, **48**, 2985 – 2995; (b) Y. You, *Curr. Opin. Chem. Biol.*, 2013, **17**, 699 – 707; (c) H. Huang, S. Banerjee and P. J. Sadler, *ChemBioChem*, 2018, **19**, 1574 – 1589.
- (a) C. A. Puckett and J. K. Barton, *J. Am. Chem. Soc.*, 2009, **131**, 8738 – 8739; (b) A. Byrne, C. S. Burke and T. E. Keyes, *Chem. Sci.*, 2016, **7**, 6551 – 6562; (c) S. Ji, X. Yang, X. Chen, A. Li, D. Yan, H. Xu and H. Fei, *Chem. Sci.*, 2020, **11**, 9126 – 9133.
- (a) A. Martin, A. Byrne, C. S. Burke, R. J. Forster and T. E. Keyes, *J. Am. Chem. Soc.*, 2014, **136**, 15300 – 15309; (b) C. S. Burke, A. Byrne and T. E. Keyes, *J. Am. Chem. Soc.*, 2018, **140**, 6945 – 6955; (c) C. S. Burke, A. Byrne and T. E. Keyes, *Angew. Chem. Int. Ed.*, 2018, **57**, 12420 – 12424.
- (a) X. Ma, J. Jia, R. Cao, X. Wang and H. Fei, *J. Am. Chem. Soc.*, 2014, **136**, 17734 – 17737; (b) K. Vellaisamy, G. Li, W. Wang, C.-H. Leung and D.-L. Ma, *Chem. Sci.*, 2018, **9**, 8171 – 8177; (c) W. Wang, K.-J. Wu, K. Vellaisamy, C.-H. Leung and D.-L. Ma, *Angew. Chem. Int. Ed.*, 2020, **59**, 17897 – 17902.
- (a) N. Y. Sardesai, K. Zimmermann and J. K. Barton, *J. Am. Chem. Soc.*, 1994, **116**, 7502 – 7508; (b) M. P. Fitzsimons and J. K. Barton, *J. Am. Chem. Soc.*, 1997, **119**, 3379 – 3380; (c) F. Noor, A. Wüstholtz, R. Kinscherf and N. Metzler-Nolte, *Angew. Chem. Int. Ed.*, 2005, **44**, 2429 – 2432; (d) A. H. Day, M. H. Übler, H. L. Best, E. Lloyd-Evans, R. J. Mart, I. A. Fallis, R. K. Allemann, E. A. H. Al-Wattar, N. I. Keymer, N. J. Buurma and S. J. A. Pope, *Chem. Sci.*, 2020, **11**, 1599 – 1606; (e) D. Truong, N. Y. S. Lam, M. Kamalov, M. Riisom, S. M. F. Jamieson, P. W. R. Harris, M. A. Brimble, N. Metzler-Nolte and C. G. Hartinger, *Chem. Eur. J.*, 2022, **28**, e202104049.
- (a) H.-Y. Shiu, H.-C. Chong, Y.-C. Leung, T. Zou and C.-M. Che, *Chem. Commun.*, 2014, **50**, 4375 – 4378; (b) A. Leonidova, V. Pierroz, L. A. Adams, N. Barlow, S. Ferrari, B. Graham and G. Gasser, *ACS Med. Chem. Lett.*, 2014, **5**, 809 – 814; (c) T. Wang, N. Zabarska, Y. Wu, M. Lamla, S. Fischer, K. Monczak, D. Y. W. Ng, S. Rau, T. Weil, *Chem. Commun.*, 2015, **51**, 12552 – 12555; (d) L. C.-C. Lee, A. W.-Y. Tsang, H.-W. Liu and K. K.-W. Lo, *Inorg. Chem.*, 2020, **59**, 14796 – 14806; (e) P. K.-K. Leung, L. C.-C. Lee, T. K.-Y. Ip, H.-W. Liu, S.-M. Yiu, N. P. Lee and K. K.-W. Lo, *Chem. Commun.*, 2021, **57**, 11256 – 11259.
- (a) K. K.-W. Lo, D. C.-M. Ng and C.-K. Chung, *Organometallics*, 2001, **20**, 4999 – 5001; (b) K. K.-W. Lo, C.-K. Chung, D. Chun-Ming Ng and N. Zhu, *New J. Chem.*, 2002, **26**, 81 – 88; (c) K. K.-W. Lo, W.-K. Hui, D. C.-M. Ng and K.-K. Cheung, *Inorg. Chem.*, 2002, **41**, 40 – 46; (d) K. K.-W. Lo, C.-K. Chung, T. K.-M. Lee, L.-H. Lui, K. H.-K. Tsang and N. Zhu, *Inorg. Chem.*, 2003, **42**, 6886 – 6897.
- K. Suzuki, A. Kobayashi, S. Kaneko, K. Takehira, T. Yoshihara, H. Ishida, Y. Shiina, S. Oishi, S. Tobita, *Phys. Chem. Chem. Phys.*, 2009, **11**, 9850 – 9860.
- García-Fresnadillo, Y. Georgiadou, G. Orellana, A. M. Braun and E. Oliveros, *Helv. Chim. Acta.*, 1996, **79**, 1222 – 1238.
- Z. Li, R. Zhao, X. Wu, Y. Sun, M. Yao, J. Li, Y. Xu and J. Gu, *FEBS J.*, 2005, **19**, 1978 – 1985.
- A. K. Varkouhi, M. Scholte, G. Storm and H. J. Haisma, *J. Control. Release.*, 2011, **151**, 220 – 228.
- (a) I. Genta, E. Chiesa, B. Colzani, T. Modena, B. Conti and R. Dorati, *Pharmaceutics*, 2018, **10**, 2 – 15; (b) M. A. Sandoval, B. R. Sloat, D. S. P. Lansakara-P, A. Kumar, B. L. Rodriguez, K. Kiguchi, J. DiGiovanni and Z. Cui, *J. Control. Release*, 2012, **157**, 287 – 296.
- The cytotoxicity data for longer incubation times (24 and 48 h) are included in the ESI.†